Int. J. Heat Mass Transfer. Vol 22, pp. 77–87

0017-9310/79/0101-0077 $02.00/0

A STEADY VORTEX DRIVEN BY A HEAT LINE SOURCE

JWO-MIN CHEN
Mechanical Engineering Department, National Tsing Hua University, Taiwan, Republic of China

and

ROBERT G. WATTS*
Institute for Energy Analysis, Oak Ridge Associated Universities, Oak Ridge, TN 37830, U.S.A.

Abstract—A mathematical analysis of a vortex that forms about a line heat source in a region with a given constant circulation far from the heat source and the ground is presented. The regions near the centerline of the vortex and near the ground, called the core and ground regions respectively, are treated separately using boundary-layer approximations. The presence of the ground induces a strong secondary flow toward the center of the vortex near the ground. The two regions are joined by matching boundary conditions through an intermediate inviscid region far from both the vortex centerline and the ground, and by matching the volume flow rates inward near the ground boundary layer and upward in the core region. The ground boundary layer has a strong effect on the core region flow. The effect appears to increase as viscosity decreases. The results are used to estimate the intensity of the energy source necessary to provide enough energy to drive a tornado. The results should also be useful in analyzing such phenomena as fire-whirls and electrically driven laboratory vortices.

NOMENCLATURE

- b, parameter defining the width of the line heat source;
- F, reduced vertical velocity function;
- f, ζ-derivative of F;
- G, reduced radial velocity function;
- g, ζ-derivative of G;
- H, reduced tangential velocity function of the ground region and reduced vertical velocity function of the core region;
- h, ζ-derivative of H;
- J, reduced function of G and H in core region, equation (3.12a);
- k, thermal conductivity;
- n, exponent in the pseudo-similarity variables η and ζ;
- p, pressure;
- P, reduced pressure;
- $\dot{Q}'''$, volumetric line heat source;
- $\dot{Q}'$, line heat source per unit length;
- r, radial coordinate;
- s, reduced function of b, equation (2.6);
- T, temperature;
- u, radial velocity;
- U, ru;
- v, tangential velocity;
- w, vertical velocity;
- W, rw;
- y, extended coordinate, $y = z + z_c$;
- z, vertical coordinate.

Greek symbols

- θ, reduced temperature;
- κ, thermal diffusivity;
- η, pseudo-similarity variable;
- ξ, similarity variable;
- ζ, pseudo-similarity variable;
- Γ_∞, circulation far from the vortex;
- γ, rv;
- ν, kinematic viscosity;
- ε, small parameter;
- δ, boundary-layer thickness of ground region;
- ξ_c, similarity variable using extended axial coordinate.

Subscripts

- 1, dimensional values;
- 0, nondimensional values;
  no subscript is used for stretched variables.

1. INTRODUCTION

VORTICES that form about concentrated heat sources are important in a variety of contexts. An example that comes to mind immediately is the fire-whirl. When a local point of intensity occurs in a ground fire, perhaps a tree or bush in a burning field, the more intense upflow and the resulting convergence causes vorticity to concentrate along a vertical line above the "hot spot". The flame is stabilized along the axis of the vortex and intensifies, extending high above the ground along the vortex axis.

We became interested in this problem for a different reason. We are investigating the possibility

*On leave of absence from: Department of Mechanical Engineering, Tulane University, New Orleans, LA 70118, U.S.A.

that thunderstorm electricity can play a role in the generation of tornadoes. It is widely believed that the enormous energy required to drive a tornado comes from the release of latent heat from moist air drawn upwards in the tornado core. However, Vonnegut [1] has suggested that tornadoes may derive at least a portion of their energy from another source. It has been suggested by Vonnegut that electrical discharges may provide such a source.

The idea of electrically driven tornadoes is obviously speculative. The fact that intense lightning generally accompanies tornado-producing weather patterns by no means proves the two phenomena depend on one another in any way. It has been shown, however, that miniature whirlwinds driven by electrical discharges can be created in the laboratory. One objective here is to model the phenomenon mathematically, so that we can discover just how much electrical power is necessary to drive a large atmospheric vortex. The model also serves as an analytical description of certain laboratory vortices created by electrical discharges such as those produced by Wilkins [2], Ryan and Vonnegut [3], and Watkins [4].

The first experimental verification that laboratory vortices could be used to stabilize discharges was published by Vonnegut, Moore and Harris [5]. Subsequently, there have been a number of studies of such vortices. Wilkins [2] investigated the swirling flow velocity distribution about an electrical arc that he produced in a 25 cm dia Plexiglas cylinder 25 cm high. The cylinder had a 10 cm dia orifice at the top through which air was drawn by a blower. Air entered the cylinder through vanes in the cylinder walls. The vanes directed the inflow air so that it had a tangential component to supply circulation. The air then swirled into the center of the cylinder and upwards out of the orifice at the top. A continuous electrical arc could be maintained between electrodes located about 18 cm apart at the top and bottom of the vortex, but a strong vortex had to be initiated by drawing air out the top with the blower before the electrical arc could be stabilized along the vortex axis.

Ryan and Vonnegut [3] later reported experimental evidence that a vortex could be generated and maintained by electrical heating from the arc alone. The maintenance of an updraft by an external blower was not necessary. Ryan and Vonnegut used two different kinds of experimental arrangements to generate their vortices. In one case the circulation was provided by admitting the air to the vortex chamber through louvres in a manner similar to the experiments of Wilkins. In another case the vortex was created along the axis of a rotating hardware cloth cage. The air converged about the arc as it passed through the hardware cloth and was given a tangential velocity component. In each case the buoyancy was produced by electrical heating of air by the arc. Vortex stabilized arcs about 1 m in height could be maintained.

Watkins [4] studied the electrical properties of arcs created in the manner of Vonnegut and his colleagues. He determined that the voltage gradient along the arc (and so the heat generation rate gradient) was independent of vertical position.

In this paper we report results of a mathematical model of the swirling flow about a line heat source. The results are used to estimate the strength and frequency of the electrical discharges necessary to drive a mature tornado. These estimates are compared with those published by Watkins [4].

2. MATHEMATICAL FORMULATION OF THE PROBLEM

2.1. *Problem statement*

Consider the three-dimensional flow in a tornado-like vortex, with a core region of large vorticity and an outer region where the circulation, Γ_∞, is constant. Whether the strong vortex is produced and maintained by an externally applied suction, as in the experiments of Ying and Chang [6] and Wei [7], or through thermal convection, the velocity field in an inviscid region far from the ground and from the vortex center is dominated by the tangential velocity. The balance of forces there is characterized by a balance between the radial pressure gradient and the centrifugal force. Near the center line of the vortex, and near the lower boundary, friction plays an important role. The objective of this research is to obtain a mathematical solution of the equations of motion and energy for an intense vortex driven by a line heat source. The work presented here is different from other research on buoyancy driven vortices that currently appears in the literature in two important ways. These are the following: 1. The vortex in this study is driven by buoyant forces created by a line heat source. 2. The present study will take account of viscous forces near the vortex centerline and also near the lower boundary (ground). Most analyses neglect the effects of viscous forces at the lower boundary. Including the ground layer in the model allows the effect of the intense inflow near the ground that occurs in real tornadoes to be included in the model.

2.2. *Governing equations*

The components of the dimensionless momentum equation in cylindrical coordinates for steady, axisymmetric flow can be written as follows:

$$U_0(U_0)_{r_0} + W_0(U_0)_{z_0} - \frac{U_0^2+\gamma_0^2}{r_0} = -r_0^2(p_0)_{r_0} + \varepsilon\left[r_0^2\left(\frac{1}{r_0}U_{0_{r_0}}\right)_{r_0} + r_0(U_0)_{z_0z_0}\right] \quad (2.1)$$

$$U_0(\gamma_0)_{r_0} + W_0(\gamma_0)_{z_0} = \varepsilon r_0\left[(\gamma_0)_{r_0r_0} - \frac{1}{r_0}(\gamma_0)_{r_0} + (\gamma_0)_{z_0z_0}\right] \quad (2.2)$$

$$U_0(W_0)_{r_0}+W_0(W_0)_{z_0}-\frac{U_0W_0}{r_0}$$
$$=\varepsilon\left\{r_0\left[r_0\left(\frac{W_0}{r_0}\right)_{r_0}\right]_{r_0}+r_0(W_0)_{z_0z_0}\right\}$$
$$+r_0^2T_0-r_0^2(p_0)_{z_0} \quad (2.3)$$

$$U_0(T_0)_{r_0}+W_0(T_0)_{z_0}$$
$$=\varepsilon[(r_0T_{0r_0})_{r_0}+r_0(T_0)_{z_0z_0}]$$
$$+\frac{r_0}{s(z_0)^{1/2}}\exp[-r_0^2/s(z_0)^{1/2}\varepsilon] \quad (2.4)$$

$$(U_0)_{r_0}+(W_0)_{z_0}=0. \quad (2.5)$$

Subscripts r_0 and z_0 refer to differentiation with respect to these variables.

The following dimensionless quantities have been defined:

$$u_0=r_1u/LU_c,\quad \gamma_0=r_1v/LU_c,\quad W_0=r_1w/LU_c,$$
$$L^3=k\Gamma_\infty^2/4g\beta\dot{Q}'\pi,\quad p_0=(p-p_\infty)/\rho U_c^2,\quad T_0=T/\Delta T,$$
$$\Delta T=\dot{Q}'/\pi k,\quad s=b/\varepsilon L^{3/2},\quad r_0=r_1/L, \quad (2.6)$$
$$z_0=z_1/L,\quad \varepsilon=2\pi\nu/\Gamma_\infty=2\pi\kappa/\Gamma_\infty,\quad U_c=\Gamma_\infty/2\pi L,$$
$$\kappa=k/\rho c_p.$$

In these expressions, u, v, and w are the radial, tangential, and vertical velocities, p is the pressure, β is the coefficient of volumetric thermal expansion, c_p is the constant pressure specific heat, k is the thermal conductivity, and T is the difference between the local temperature and that far from the vortex. Property values are assumed to be constants with the exception of the density, which is allowed to vary only in the body force term in accordance with the Boussinesq approximation. The application of this approximation to atmospheric systems was discussed by Spiegel and Veronis [8]. Although it may not be entirely accurate for the description of tornadoes, it is certainly accurate for fire whirls and for laboratory vortices.

We have postulated a heat source term of the special form:

$$\dot{Q}'''=\frac{\dot{Q}'}{\pi(z_1)^{1/2}b}\exp[-r_1^2/b(z_1)^{1/2}] \quad (2.7)$$

where $\dot{Q}'$ is the rate at which heat is emitted from the source per unit height above the lower surface and b is an adjustable constant. This heat source term displays the important property that

$$\int_0^\infty \dot{Q}'''(r_1,\theta_1,z_1)2\pi r_1\,dr_1=\dot{Q}'(z_1). \quad (2.8)$$

$\dot{Q}'(z_1)$ can be chosen to be any function of height above the lower bounding surface. By choosing various values of b a narrow or wide heat generating region can be created while keeping $\dot{Q}'(z_1)$, the vertical gradient of the heat generation rate, constant. By choosing b to be sufficiently small, a line heat source can be approximated. We shall assume henceforth that $\dot{Q}'$ is a constant.

The boundary conditions are expressed as:

$$U_0(0,z_0)=\gamma(0,z_0)=(W_0)_{r_0}(0,z_0)=(T_0)_{r_0}(0,z_0)=0$$
$$\lim_{r_0\to\infty}\gamma_0=1,\quad \lim_{r_0\to\infty}(U_0 \text{ and } W_0) \text{ are bounded.} \quad (2.9)$$
$$U_0(r_0,0)=\gamma_0(r_0,0)=W_0(r_0,0)=0.$$

2.3. *Boundary layers*

When ε is small, it is anticipated that the solution of (2.1)–(2.5) will yield a narrow vortex along the vertical axis with a shallow region of strong inflow near the lower boundary. Outside these two boundary-layer regions the effects of viscous force terms (terms multiplied by ε) should be small, and the flow characteristic of an inviscid vortex. The parameter ε may be thought of as the inverse of a Reynolds number since $\varepsilon=2\pi\nu/\Gamma_\infty=\nu/U_cL$.

The flow in atmospheric vortices such as tornadoes and dust devils is undoubtedly turbulent, as was the flow in both the core and the ground boundary layers of the laboratory vortices of Wei [7] and Ying and Chang [6]. In previous studies of atmospheric vortices (for example, Kuo [9, 10], Serrin [11], Gutman [12], Mal'bakhov [13]), the viscosity has been treated as a constant, and some appropriate value for eddy viscosity used to estimate numerical results. The same policy will be adopted here. It should be pointed out that the appropriate eddy viscosity may be different for the region near the vortex and the region near the ground.

3. THE CORE REGION

Kuo [9] used a value of $5\,m^2s^{-1}$ for ν in the region near $r_0=0$. Serrin [11] suggested that the turbulence level in this region is self-regulating and the $\nu=0.1\Gamma_\infty/2\pi$. Gutman [12] used $10\,m^2s^{-1}$. Mal'bakhov [13] used $100\,m^2s^{-1}$. All these studies were concerned with real tornadoes (rather than laboratory models).

When the value of $\Gamma_\infty=47\times10^3\,m^2s^{-1}$ observed by Lewis and Perkins [14] near the Cleveland tornado is used, it is seen that ε ranges between approximately 0.1 (Serrin's value) and 0.67×10^{-3} (Kuo's value). It may therefore be considered to be much smaller than unity. The boundary-layer character of the solution referred to above can therefore be anticipated. With this in mind, three regions will be considered separately; the region near the vortex centerline (core region), the region near the ground and away from the centerline (ground region), and the "inviscid" region far from both core and ground.

3.1. *Boundary-layer equations*

It is expected that in the core region the upward velocity is strong within a relatively narrow region where viscous effects are important. Using boundary-layer arguments, it can easily be shown that when terms of order of magnitude ε are neglected compared with terms of order unity in (2.1)–(2.5) the

following equations result:

$$\gamma^2 = r^3 p_r \tag{3.1}$$

$$U\gamma_r + W\gamma_z = r\left(\gamma_{rr} - \frac{\gamma_r}{r}\right) \tag{3.2}$$

$$rU(W/r)_r + WW_z = r^2 T + r[r(W/r)_r]_r \tag{3.3}$$

$$UT_r + WT_z = (rT_r)_r + \frac{r}{s(z)^{1/2}} \exp[-r^2/s(z)^{1/2}] \tag{3.4}$$

$$U_r + W_z = 0 \tag{3.5}$$

where $r = r_0/(\varepsilon)^{1/2}$, $z = z_0$, $U = U_0/\varepsilon$, $\gamma = \gamma_0$, $W = W_0/(\varepsilon)^{1/2}$ and $p = p_0\varepsilon$ are reduced variables.

Equations (3.1)–(3.5) are accurate precisely where one would expect boundary-layer equations to be accurate. They are not expected to be accurate near $z = 0$, for example, where the axial pressure gradient, as well as other terms, might be large.

The boundary conditions are

$$\begin{gathered} U(0, z) = \gamma(0, z) = W_r(0, z) = T_r(0, z) = 0 \\ W(\infty, z) = T(\infty, z) = p(\infty, z) = 0 \\ \gamma(\infty, z) = 1. \end{gathered} \tag{3.6}$$

3.2. *Similarity variables*

Equations (3.1)–(3.5) can be reduced to a set of ordinary differential equations if the following changes of variables are made:

$$\begin{gathered} U = G(\xi),\ \gamma = \gamma(\xi),\ T = \theta(\xi),\ \xi = r/z^{1/4} \\ P = z^{1/2} p(\xi),\ W = 4z^{3/4} H(\xi). \end{gathered} \tag{3.7}$$

When the variables defined by (3.7) are substituted into (3.1) through (3.5), the resulting ordinary differential equations are as follows:

$$\gamma^2 = \xi^3 p' \tag{3.8}$$

$$\xi\gamma'' = (J+1)\gamma' \tag{3.9}$$

$$G\left[H' - \frac{H}{\xi}\right] + H(3H - \xi H') = \frac{\xi^2}{4}\theta + \xi\left(\frac{H}{\xi^2} - \frac{H'}{\xi} + H''\right) \tag{3.10}$$

$$G\theta' - \xi H\theta' = \xi\theta'' + \theta' + \frac{\xi}{s}\exp\left(-\frac{\xi^2}{s}\right) \tag{3.11}$$

$$J' = -4H \tag{3.12}$$

where:

$$J = G - \xi H. \tag{3.12a}$$

The boundary conditions (3.6) require that

$$\begin{gathered} G(0) = \gamma(0) = 0 \\ H'(0) = \theta'(0) = 0 \\ \gamma(\infty) = 1 \\ H(\infty) = \theta(\infty) = P(\infty) = 0. \end{gathered} \tag{3.13}$$

Direct integration using the fourth-order Runge–Kutta method along with a "shooting method" was used to obtain solutions to the equations.

3.3. *Solution and results*

Equations (3.8)–(3.13) were solved for several values of the parameter s. The parameter s is directly proportional to b, the parameter that determines the width of the heat source at a given height. Solutions were obtained for $s = 10, 5, 1, 0.1$, and 0.01.

The results are shown in Figs. 1–3. The dimensionless circulation and temperature are plotted against the independent variables ξ in Fig. 1. Figure 2 shows the dimensionless variables J and H.

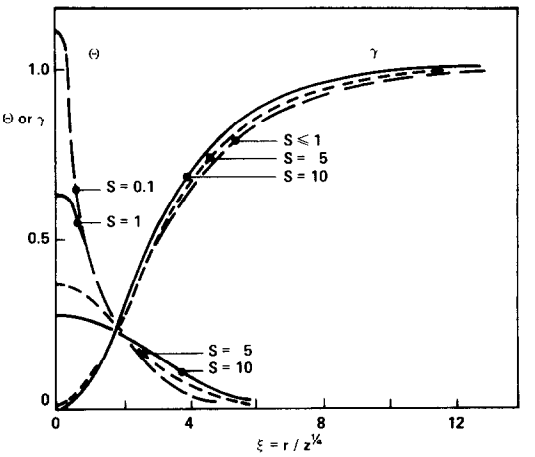

FIG. 1. Reduced potential temperature and reduced circulation in the core region.

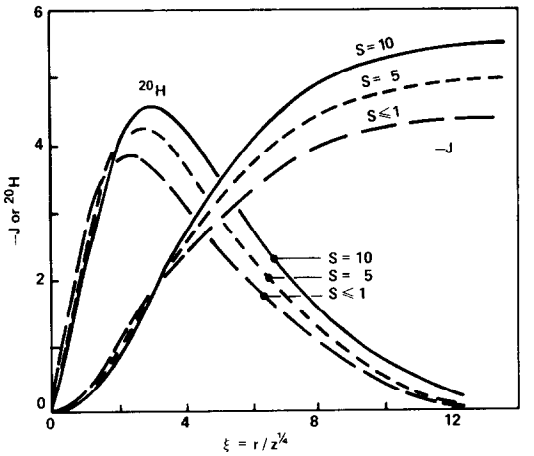

FIG. 2. Reduced vertical and radial velocity. Functions in the core region.

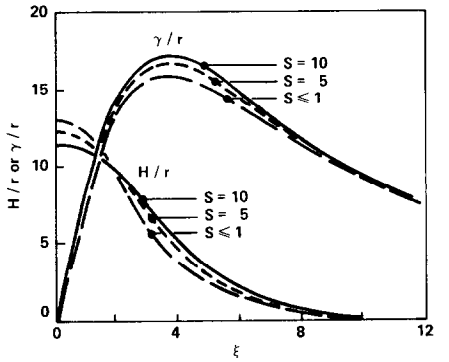

FIG. 3. Reduced tangential velocity and H/r in the core region.

The dimensionless tangential velocity and the vertical velocity variable H/r are shown if Fig. 3. Some variation with s is seen to occur when $s > 1$. At smaller values of s the variation in any of the dimensionless variables except the dimensionless temperature is imperceptible when s decreases. Hence, for all the flow parameters it can be assumed that values of the parameters when $s < 1$ adequately represent the swirling flow about a line heat source.

The peak value of upward speed w_1 is

$$w_{1,\max} = \frac{2C_1 z^{1/2}}{\pi}\left(\frac{4\beta g\pi\dot{Q}'}{k}\right)^{1/2}. \quad (3.14)$$

The radial position where the maximum tangential speed occurs is

$$r_{1,\max} = C_2 \nu^{1/2}\left(\frac{kz_1}{4\pi g\beta\dot{Q}'}\right)^{1/4} \quad (3.15)$$

and the value of the maximum tangential speed is

$$v_{1,\max} = \frac{C_3\Gamma_\infty}{2\pi C_2\nu^{1/2}}\left(\frac{4\beta g\dot{Q}'}{kz_1}\right)^{1/4}. \quad (3.16)$$

The total upward volume flow induced by the heat source is proportional to the value of G far from the heat source. This can be shown by writing the continuity equation for a cylindrical control volume about the vortex centerline and allowing the radius R to approach infinity.

When

$$s < 1, \quad \lim_{r\to\infty} ru = \lim_{\xi\to\infty} G(\xi) = -4.35. \quad (3.17)$$

Thus, the upward volume flow rate for the case of a line heat source is

$$\dot{m}_{up}/\rho = 2\pi(4.35)\nu z_1. \quad (3.18)$$

The volume flow rate increases linearly with the distance z_1 above the ground and the kinematic viscosity as more and more air is drawn into the vortex.

4. THE GROUND BOUNDARY LAYER

An approximate solution of the equations that describe the flow in the boundary layer near the ground is presented in this section. As was the case with the core region equations, certain terms can be shown to be negligible at a reasonable distance from the origin when $\varepsilon \ll 1$. However, we have not been able to discover a suitable similarity variable for this set of differential equations. Nonlinear partial differential equations must be solved.

A technique called the local nonsimilarity method described by Sparrow and Yu [15] is used to obtain approximate solutions. A detailed discussion of the accuracy of the method together with details of the computations has been given by Chen [16].

4.1. *Boundary-layer equations*

The flow in the boundary layer near the ground is expected to be vigorously inward. It is therefore expected that U and γ will be of order unity while W will be considerably smaller. When terms of order ε are neglected, the equations governing the flow in the region near the ground are as follows:

$$UU_r + WU_z - (U^2+\gamma^2)/r = -r^2 p_r + rU_{zz} \quad (4.1)$$

$$U\gamma_r + W\gamma_z = r\gamma_{zz} \quad (4.2)$$

$$U_r + W_z = 0 \quad (4.3)$$

where $r = r_0$, $z = z_0/(\varepsilon)^{1/2}$, $\gamma = \gamma_0$, $U = U_0$, $W = W_0/(\varepsilon)^{1/2}$, and $p = p_0$.

The velocity is required to be zero at the ground ($z = 0$). The radial velocity far above the ground is that induced in the inviscid region by the core region flow. Thus, the mathematical boundary conditions are as follows:

$$\begin{aligned} U(r,0) = \gamma(r,0) = W(r,0) = 0, \\ U(r,\infty) = \varepsilon G(\infty), \quad \gamma(r,\infty) = 1. \end{aligned} \quad (4.4)$$

4.2. *Solution of the equations*

Discussion of some characteristics of these nonlinear partial differential equations is facilitated under a change of variables. Let

$$\begin{aligned} \eta = zr^{(n-1)/2}, \quad \zeta = r^{(n+1)/2} \\ U = r^{(n+1)}G(\eta,\zeta), \quad W = r^{(n+1)/2}F(\eta,\zeta) \\ \gamma = r^{(n+1)}H(\eta,\zeta). \end{aligned} \quad (4.5)$$

When these definitions are substituted into (4.1)–(4.4), there results the equivalent set of partial differential equations.

$$F_\eta + (n+1)G + \left(\frac{n-1}{2}\right)\eta G_\eta = \left(\frac{n+1}{2}\right)\zeta G_\zeta \quad (4.6)$$

$$-G_{\eta\eta} + nG^2 + \left[\left(\frac{n-1}{2}\right)\eta G + F\right]G_\eta - H^2 + \frac{1}{\zeta^2} = -\left(\frac{n+1}{2}\right)\zeta G G_\zeta \quad (4.7)$$

$$-H_{\eta\eta} + (n+1)GH + \left[\left(\frac{n-1}{2}\right)\eta G + F\right]H_\eta = -\left(\frac{n+1}{2}\right)\zeta G H_\zeta \quad (4.8)$$

with boundary conditions,

$$\begin{aligned} F(0,\zeta) = G(0,\zeta) = H(0,\zeta) = 0, \\ G(\infty,\zeta) = U_b/\zeta^2, \quad H(\infty,\zeta) = 1/\zeta^2. \end{aligned} \quad (4.9)$$

Examination of (4.6)–(4.9) reveals that when $n = -1$, the set of partial differential equations reduces to a set of ordinary differential equations. The independent variable is $\eta = z/r$. Therefore, $\eta = z/r$ is a similarity variable.

The set of equations that results has been studied by Goldshtik [17] and found to have no solution satisfying the boundary conditions (4.9). It is easily seen that this is the only choice of n that reduces (4.6)–(4.8) to a set of ordinary differential equations. It is, of course, possible that a similarity variable of more complex form might exist. Such a similarity variable has not been found. The boundary-layer profiles must therefore be treated as being nonsimilar.

There are a number of techniques that have been used with some success to obtain approximate solutions for non-similar boundary layers (see Rosenhead [18]). The simplest approach is through the assumption of local similarity. The terms on the RHS of (4.6)–(4.8) are assumed to be negligibly small so that the differential equations can be treated formally as ordinary differential equations and integrated over η at particular values of ζ. The obvious advantage of this method is its computational simplicity. An improved technique has been presented by Sparrow and Yu [15]. In this technique the terms on the RHS of (4.6)–(4.8) are not assumed to be zero, but are estimated instead. To accomplich this the terms G_ζ, H_ζ and F_ζ are written as g, h and f. Thus (4.6), (4.7) and (4.8) become

$$F_\eta = -(n+1)G - \left(\frac{n-1}{2}\right)\eta G_\eta - \left(\frac{n+1}{2}\right)\zeta g \quad (4.10)$$

$$G_{\eta\eta} = nG^2 + \left[\left(\frac{n-1}{2}\right)\eta G + F\right]G_\eta - H^2 + \frac{1}{\zeta^2} + \left(\frac{n+1}{2}\right)\zeta G g \quad (4.11)$$

$$H_{\eta\eta} = (n+1)GH + \left[\left(\frac{n-1}{2}\right)\eta G + F\right]H_\eta + \left(\frac{n+1}{2}\right)\zeta G h. \quad (4.12)$$

Differential equations for g, h and f can be obtained by differentiating (4.10), (4.11), and (4.12) with respect to ζ. The equations that result are

$$f_\eta = -(n+1)g - \left(\frac{n-1}{2}\right)\eta g_\eta - \left(\frac{n+1}{2}\right)g - \left(\frac{n+1}{2}\right)\zeta g_\zeta \quad (4.13)$$

$$g_{\eta\eta} = 2ngG + \left[\left(\frac{n-1}{2}\right)\eta g + f\right]G_\eta + \left[\left(\frac{n-1}{2}\right)\eta G + F\right]g_\eta - 2hH + \left(\frac{n+1}{2}\right)gG + \left(\frac{n+1}{2}\right)\zeta g^2 + \left(\frac{n+1}{2}\right)\zeta G g_\zeta \quad (4.14)$$

$$h_{\eta\eta} = (n+1)gH + (n+1)Gh + \left[\left(\frac{n-1}{2}\right)\eta g + f\right]H_\eta + \left(\frac{n+1}{2}\right)\zeta g h + \left[\left(\frac{n-1}{2}\right)\eta G + F\right]h_\eta + \left(\frac{n+1}{2}\right)Gh + \left(\frac{n+1}{2}\right)\zeta G h_\zeta \quad (4.15)$$

The assumption is now made that g_ζ, h_ζ and f_ζ are small enough to be neglected. Physically, this corresponds to estimating the values of G_ζ, H_ζ and F_ζ at a given value of ζ under the assumption that although G, H and F vary with ζ, the second derivatives of these terms are locally small.

The set of equations that results is a set of ordinary differential equations. Hence, the equations can be integrated using the same well-known schemes that are used when similarity variables are found. An improvement in the accuracy of the method can be sought by defining new variables for g_ζ, h_ζ and f_ζ differentiating again with respect to ζ, and neglecting the terms $g_{\zeta\zeta}$, $h_{\zeta\zeta}$ and $f_{\zeta\zeta}$. The computational appeal of the technique fades rather quickly as computer time and memory requirements mount, however. Sparrow and Yu [15] and Sparrow and Minkowycz [19] have obtained spectacular accuracy in certain applications by differentiating only once.

With g_ζ, h_ζ and f_ζ set equal to zero, (4.10)–(4.15) have been solved consistent with the boundary conditions:

$$F(0,\zeta) = G(0,\zeta) = H(0,\zeta) = f(0,\zeta) = g(0,\zeta) = h(0,\zeta) = 0$$
$$G(\infty,\zeta) = U_b\zeta^{-2}, \quad H(\infty,\zeta) = \zeta^{-2},$$
$$g(\infty,\zeta) = -2U_b\zeta^{-3}, \quad h(\infty,\zeta) = -2\zeta^{-3}. \quad (4.16)$$

U_b is -4.35ε. Solutions were carried out for $\varepsilon = 0.01$ and 0.67×10^{-3}, and for the special case of $n = 1$. This value of n was used strictly for convenience. The variable η reduces to z for this case, and a number of terms drop out of (4.10)–(4.15). Exact values of γ, U and W obtained by solving equations (4.6)–(4.8) are independent of the choice of n. A partial test of the accuracy of the solutions of equations (4.10)–(4.15) for $n = 1$ can be obtained by comparing these results to those for some other choice of n. Such a comparison is given in Fig. 4 for the cases of $r = 5$, $r = 7$ and $\varepsilon = 0.01$. The qualitative agreement is excellent, although slightly higher radial velocities result from $n = 0.5$.

Using $n = 1$, equations (4.10)–(4.16) have been solved for the radial positions $r = 3$, $r = 5$ and $r = 7$ for $\varepsilon = 0.01$ and for $r = 4$, 5 and 7 for $\varepsilon = 0.67$

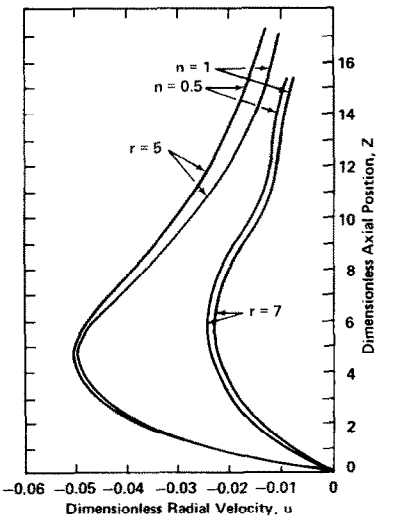

FIG. 4. Comparison of radial velocity profile near the ground, $\varepsilon = 0.01$, various n and r.

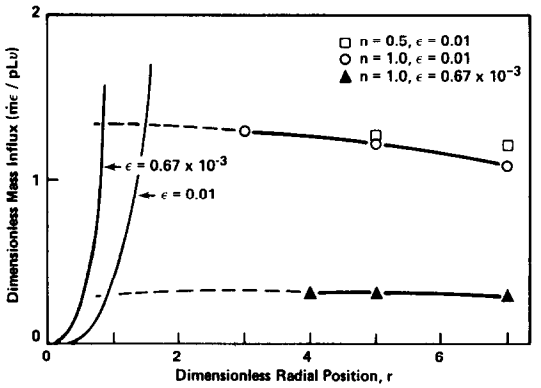

FIG. 5. Dimensionless mass flux in the ground boundary layer and in the core.

$\times 10^{-3}$. The radial mass flow rates in the boundary layer are shown plotted as a function of radial position in Fig. 5. The upper edge of the boundary layer is defined as that position where the radial velocity is within 2% of the value in the inviscid region. The radial volume flow rate for the case of $n = 0.5$, for $r = 5$ and $r = 7$ is also shown for comparison for $\varepsilon = 0.01$.

As another test of the accuracy of the method, the maximum value of g was determined at various values of radial position. The results are shown plotted as Fig. 6. The values of g, and incidentally, of g_ζ are small at values of r greater than about 3 for $\varepsilon = 0.01$ and 4 for $\varepsilon = 0.67 \times 10^{-3}$. At smaller values of r, the method does not yield accurate results. An improved solution, accurate for smaller values of r, is presently being developed and will be published in the future.

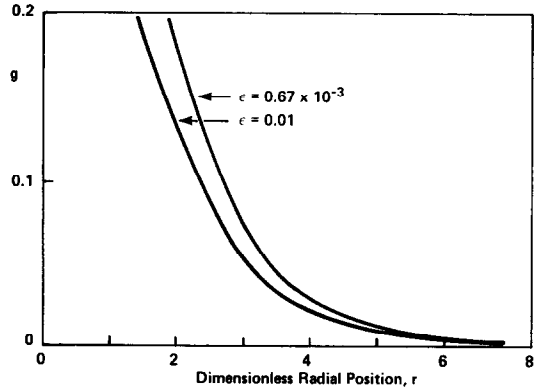

FIG. 6. Variation of the variable $g = G_\zeta$ with radial position.

4.3. *Remarks concerning accuracy of the results*

When the approximate solution is accomplished, the results are slightly different for the cases of $n = 1$ and $n = 0.5$. However, the qualitative agreement between the two is excellent, and the quantitative agreement is satisfactory, especially as regards the value of the volume inflow rate. While greater accuracy is always desirable, it must be pointed out that attempts to obtain extreme accuracy in computations involving weather phenomena such as tornadoes may not actually improve the agreement between the theoretical model and the natural phenomenon. The reason for this is that the values of certain quantities such as the turbulent viscosity are not well known. Thus, the accuracy of the results reported in this chapter can be safely regarded as being at least as accurate as the knowledge of the viscosity.

5. MATCHING THE REGIONS

5.1. *The technique used*

The solution of the core region must now be matched with the solution for the ground region in such a way that the mutual interaction of the regions is taken into account. The vortex affects the ground region by creating the pressure gradient that causes the strong inflow in the ground boundary layer. The mass influx from this layer erupts near the center, causing a large vertical velocity at the base of the core region.

The approximate matching of the core and ground regions is accomplished in four steps. (1) It is first demonstrated that the substitution $y_1 = z_1 + z_{c1}$, z_{c1} = constant, leaves the differential equations of momentum, continuity and energy for the core region unchanged if the heat source term is changed to $\dot{Q}''' = [\dot{Q}'/\pi b(y_1)^{1/2}]\exp[-r_1^2/b(y_1)^{1/2}]$. The similarity variable $\xi_c = r/y^{1/4}$ then reduces the system of partial differential equations to ordinary differential equations as before. Here $y = y_1/L$. (2) The dimensionless vertical velocity in the core region at $z_1 = 0$ is now not zero, but is given by $rw = 4(z_{c1}/L)^{3/4}\varepsilon^{1/2}H(\xi_c)$. The dimensionless volume flow rate upwards in the core region at $z_1 = 0$ is $\dot{m}\varepsilon/\rho\nu L = 4.35 \times 2\pi(z_{c1}/L)$. The dimensionless volume flow rate inward in the ground boundary layer is shown in Fig. 5 for the cases of $\varepsilon = 0.01$ and 0.67×10^{-3}. The dimensionless height $(z_{c1} + \delta_1)/L$ is chosen so that these mass flow rates balance. This amounts to assuming that the effect of the mass influx due to the ground can be modelled by an equivalent imaginary heat source that extends below the ground. This is an approach similar to that taken by Turner [20] in modelling the effect of the lower surface on laboratory vortices. (3) The question of whether the shape of the vertical velocity profile induced by the equivalent heat source matches that resulting from the eruption of the inward flow is only briefly addressed. (4) Finally, the effect on the core region solution of the weak downdraft at large radial positions induced by the ground boundary layer is shown to be very small.

5.2. *Matching the mass flow rates*

When the substitution $y = z + (z_{c1}/L)$ is made in (3.1)–(3.5) and the heat source term is written as

$$\dot{Q}''' = [\dot{Q}'/\pi b(y_1)^{1/2}]\exp[-r_1^2/b(y_1)^{1/2}]$$

the following equations result:

$$\gamma^2 = r^3 p_r \tag{5.1}$$

$$U\gamma_r + W\gamma_y = r\left[\gamma_{rr} - \frac{1}{r}\gamma_r\right] \tag{5.2}$$

$$rU\left(\frac{W}{r}\right)_r + WW_y = r^2 T + r\left[r\left(\frac{W}{r}\right)_r\right]_r \tag{5.3}$$

$$UT_r + WT_y = (rT_r)_r + \frac{r}{s(y)^{1/2}}\exp\left[-\frac{r^2}{s(y)^{1/2}}\right]. \tag{5.4}$$

$$U_r + W_y = 0. \tag{5.5}$$

Equations (5.1)–(5.5) are identical to (3.1)–(3.5) except that y has replaced z. When $z > 0$ these equations together with the boundary conditions

$$U(0, y) = \gamma(0, y) = W_r(0, y) = T_r(0, y) = 0$$

$$\lim_{r\to\infty} W(r, y),\ T(r, y),\ p(r, y) = 0, \tag{5.6}$$

$$\lim_{r\to\infty} \gamma = 1$$

describe a physical situation wherein above the origin there is a vortex about a line heat source. The vertical velocity is not zero when z is zero, but is the velocity that would result from extending the heat source a distance z_c below $z = 0$.

When the similarity variables defined by (3.7) are applied (replacing z by y) the ordinary differential equations that result are the same as (3.8)–(3.12), and the boundary conditions are those given by (3.13). The solution of these equations was accomplished in Section 3.

Suppose the vertical velocity at $z = \delta_1/L = \delta$ a small distance above $z = 0$ comes not from an imaginary heat source extending below the origin, but from the negative radial velocity generated through the interaction of the potential vortex outside the core region with the ground as described in Section 4. The volume flow rates inward through the ground boundary layer and upward through the base of the core can be balanced by choosing $z_c + \delta$ properly. The bulk flow, but not necessarily the details of the velocity distributions, will then be matched.

The matching has been carried out specifically for the cases of $\varepsilon = 0.01$ and $\varepsilon = 0.67 \times 10^{-3}$. The values were chosen as being representative values for tornadoes, because they lie between the extremes used by Kuo ($\varepsilon = 0.67 \times 10^{-3}$) and by Serrin ($\varepsilon = 0.1$) and are still much smaller than unity. The volume flow rate upward in the core region is given by (3.18). The radial position marking the edge of the core boundary as defined by the location when $W = 0.01W(0, y)$ is $r_1/L = 10.4(y_1/L)^{1/4}\varepsilon^{1/2}$. Solving for y_1 and substituting it for z_1 (3.18) gives an expression for the upward volume flow rate in the core as a function of the core boundary-layer thickness. In dimensionless form,

$$\frac{\dot{m}_{up}}{\rho\nu L} = 8.7\pi\frac{(r_1/L)^4}{(10.4)^4\varepsilon} \tag{5.7}$$

When this equation is plotted in Fig. 5 for $\varepsilon = 0.01$ and $\varepsilon = 0.67 \times 10^{-3}$, the value of r at which the curves cross the radial mass flow rate curves is the core boundary-layer thickness at $z = \delta$. The corresponding value of $z_c + \delta$ can then be determined from (3.18). The value for the case of $\varepsilon = 0.01$ is $z_c + \delta = 4.3$. When $\varepsilon = 0.67 \times 10^{-3}$, the value is $z_c + \delta = 17.2$.

The determination of the crossing point for the case of $\varepsilon = 0.67 \times 10^{-3}$ requires a large extrapolation of the ground boundary-layer mass flow rate curve, while the case of $\varepsilon = 0.01$ requires only a fairly short extrapolation. It was not possible to compute values of the dimensionless mass flow rates for smaller values of radial position than those shown by the method used here because of the very large computer time and memory requirements. It was pointed out in Section 4 that the value of g (the term neglected in the two equation group calculation procedure) becomes very large when r is small. A three or four equation group technique may be required for analytical investigation of the flow behavior at small values of r. Experimental data of Wei [7] and of Ying and Chang [6] as well as the computations for $\varepsilon = 0.01$ support the contention that the boundary-layer thickness and the inflow within the boundary layer remain very nearly constant until the tangential velocity begins to depart from the potential flow values. At that point the flow begins to erupt upwards into the vortex core. While both experimental data and analytical results for the larger values of ε indicate that the extrapolation is reasonably accurate, the value of $z_c + \delta$ for this case must be used with some care.

5.3. *Remarks about the upflow near the axis*

In the region near the axis the flow above the ground is nearly solid body rotation. At larger values of radial position the tangential velocity reaches a maximum value, and finally approaches $\Gamma_\infty/2\pi r$, the potential flow value. Experimental results of Turner [20] as well as the approximate analyses of Kuo [10] and Carrier *et al.* [21] indicate that the region of upflow from the boundary layer beneath a combined Rankine vortex extends approximately to the radial location where the tangential velocity first departs appreciably from potential flow. In particular, the experiments of Turner [20] show a bell-shaped axial velocity profile with strong upflow near the center. The velocity becomes weakly negative at approximately twice the radius of maximum tangential velocity. Kuo [10], on the other hand, predicts a maximum vertical velocity slightly away from the axis. The velocity then decreases and becomes weakly negative in the potential flow region. It may be anticipated that the details of the vertical velocity distribution at the base of the core region are at least similar to the bell-shaped profile resulting from an imaginary heat source below $z = 0$. Turner [20] has reported that it is not crucial that the matching be precise in its details. Obviously, the region very close

to the origin is not accurately modelled in this paper. The full Navier–Stokes equations must be used in that region. It is indeed a most interesting region, but its analysis must be left for future investigation.

5.4. *The effect of the weak downdraft on the core region*

In the solution of the core region equation in Section 2, it was assumed that the vertical velocity far from the axis was zero. Solution of the equations for the ground region in Section 4 indicates that outside the core region a weak downward flow is induced by the ground boundary layer. If this non-zero vertical velocity is included in the boundary conditions given by (3.6) the differential equations and boundary conditions become nonsimilar.

To investigate the possible effect of the downflow on the core region solution, the nonsimilar equations have been solved approximately using the local similarity approach. The results have been reported by Chen [16]. The core region flow is affected only very slightly.

6. SOME OBSERVATIONS ABOUT TORNADOES

In this section an estimate of the magnitude of the heat source necessary to drive a tornado is presented. Computations are performed using two values of circulation, $\Gamma_\infty = 47 \times 10^3\,\mathrm{m^2\,s^{-1}}$ and $\Gamma_\infty = 4.1 \times 10^5\,\mathrm{m^2\,s^{-1}}$. The first of these corresponds to the circulation observed by Lewis and Perkins [14] near the Cleveland tornado of 8 June, 1953 and is also very close to the value estimated by Fujita [22] for the Fargo tornado of 20 June, 1957. The second value is the value estimated by Fujita [23] for the Tecumseh, Michigan tornado. It is probably unreasonably large. The heat source is estimated using $\varepsilon = 0.67 \times 10^{-3}$ and $\varepsilon = 0.01$ for the two cases of Γ_∞.

6.1. *The method of computation*

The maximum tangential speed and the radial position where it occurs are related by

$$r_{1,\max} v_{1,\max} = 0.63\Gamma_\infty/2\pi \tag{6.1}$$

as can be seen by combining (3.15) and (3.16). The maximum velocity occurs at the base of the core region, that is, at $y = z_c + \delta$. This value is a function of ε as was seen in Section 5.

The vertical gradient of the heat generation rate $\dot{Q}'$ is obtained from the definition of L (equation 2.6).

$$\dot{Q}' = \frac{\rho c_p \nu \Gamma_\infty^2}{4\pi g \beta L^3} \tag{6.2}$$

L^3 can be eliminated from (6.2) by first noting that the velocity maximum occurs when $\xi_c = 4$ (Fig. 3). Thus,

$$L = \frac{r_{1,\max}}{4(z_c+\delta)^{1/4}\varepsilon^{1/2}}. \tag{6.3}$$

Substituting L from (6.3) and $r_{1,\max}$ from (6.1) into (6.2) and rearranging gives the following expression for $\dot{Q}'$:

$$\dot{Q}' = \frac{64\pi}{(0.63)^3}\left(\frac{\rho c_p}{\beta g}\right)\varepsilon^{5/2}(z_c+\delta)^{3/4} v_{1,\max}^3. \tag{6.4}$$

When the properties of air at standard atmospheric pressure are used

$$64\pi\rho c_p/(0.63)^3 \beta g = 1.8 \times 10^6\,\mathrm{J\,s^{-2}\,m^{-4}}. \tag{6.5}$$

6.5. *Results*

When $\Gamma_\infty = 47 \times 10^3\,\mathrm{m^2\,s^{-1}}$, and a maximum tangential speed of $82\,\mathrm{m\,s^{-1}}$, corresponding to Hoecker's [24] data, are used, the values of the radius of maximum winds and the vertical heat generation gradient are computed to be

$$r_{1,\max} = 57.6\,\mathrm{m},\ \dot{Q}' = 100\,\mathrm{kW\,m^{-1}} \text{ when } \nu = 5\,\mathrm{m^2\,s^{-1}}$$

and

$$r_{1,\max} = 57.6\,\mathrm{m},\quad \dot{Q}' = 3 \times 10^4\,\mathrm{kW\,m^{-1}} \quad \text{for } \nu = 75\,\mathrm{m^2\,s^{-1}}.$$

When $\Gamma_\infty = 4.1 \times 10^5\,\mathrm{m^2\,s^{-1}}$, the values corresponding to $v_{1,m} = 82\,\mathrm{m\,s^{-1}}$ are

$$r_{1,\max} = 795\,\mathrm{m},\ \dot{Q}' = 100\,\mathrm{kW\,m^2} \text{ for } \nu = 44\,\mathrm{m^2\,s^{-1}}$$

and

$$r_{1,\max} = 795\,\mathrm{m},\quad \dot{Q}' = 3 \times 10^4\,\mathrm{kW\,m^{-1}} \text{ for } \nu = 650\,\mathrm{m^2\,s^{-1}}.$$

The values of $r_{1,m}$ are reasonable. The last value of ν is rather large. Equation (6.5) indicates that for a given maximum velocity, the heat generation rate is a function of ε only. When ε decreases, $z_c+\delta$ increases. However, the group $\varepsilon^{5/2}(z_c+\delta)^{3/4}$ decreases rapidly as ε decreases. When $\varepsilon = 0.01$, $\varepsilon^{5/2}(z_c+\delta)^{3/4} = 3 \times 10^{-5}$ and when $\varepsilon = 0.67 \times 10^{-3}$, $\varepsilon^{5/2}(z_c+\delta)^{3/4} = 9.9 \times 10^{-8}$. Such large dependence on viscosity is unfortunate, since the value of ν is so poorly known.

6.3. *Electrical discharges*

Considering a heat source 5 km high, the heat supplied to the vortices analyzed in Section 6.2 ranges between 5×10^5 kW and 1.5×10^8 kW. Watkins [4] estimated that the power dissipated by an electrical discharge of a discrete stroke nature (such as lightning) ranges between 10^5 and 10^9 kW if repetitive strokes occur at about 10–20 strokes per s. The atmospheric static electricity effects that accompany tornadoes are well-known. It has been reported by Jones [25] that lightning discharges occur at a rate of 10–20 per s in tornado-producing thunderstorms.

7. CONCLUSIONS

In Sections 2–5 an approximate analytical solution was obtained for the swirling flow due to a line heat source in a region of strong circulation. A special feature of the model is that it takes into account the presence of the boundary layer that forms near the ground beneath the vortex. The

viscous boundary layer near the ground induces a secondary flow inward toward the centerline of the vortex. It was shown in Section 5 that the resulting volume flow rate toward the center has a strong effect on the flow in the region near the vortex.

The intensity of the line heat source required to provide the buoyant force necessary to drive an atmospheric vortex with velocities and length scales similar to those found in tornadoes was computed in Section 6. It was shown that a heat source whose magnitude ranges between 5×10^5 kW and 1.5×10^8 kW is sufficient to maintain even very large and intense tornadoes such as the Tecumseh, Michigan tornado. The values lie well within the range of the 10^5–10^9 kW estimated by Watkins [4] as being dissipated by lightning if repetitive strokes occur at 10–20 strokes per s. It must therefore be concluded that electrical discharges of a discrete nature can provide enough power to drive a tornado.

The analysis presented here should be useful in modelling other types of buoyancy-driven vortices, such as fire storms and laboratory electrical vortices such as those created by Ryan and Vonnegut [3] and by Watkins [4].

Acknowledgements—The work reported here was supported by the National Science Foundation under Grant GK-35993. A portion of the computer was provided by the Tulane University Computer Center.

REFERENCES

1. B. Vonnegut, Electrical theory of tornadoes, *J. Geophys. Res.* **65**(1) (1960).
2. E. Wilkins, The role of electrical phenomena associated with tornadoes, *J. Geophys. Res.* **69**, 2435 (1964).
3. R. T. Ryan and B. Vonnegut, Miniature whirlwinds produced in the laboratory by high-voltage electrical discharges, *Science* **168** (1970).
4. D. Watkins, The properties of a vortex-stabilized discharge in the current range of 3 to 300 amperes and an estimation of the ability of electrical discharges to power tornadoes, Ph.D. Dissertation, SUNY-Albany (1975).
5. D. Vonnegut, C. B. Moore and D. K. Harris, Stabilization of a high-voltage discharge by a vortex, *J. Meteorology* **17**, 468–471 (1960).
6. S. J. Ying and C. C. Chang, Exploratory model study of tornado-like vortex dynamics, *J. Atmos. Sci.* **27**, 1–14 (1970).
7. S. M. Wei, Experimental investigation of the ground boundary layer of a tornado-like vortex, M.S. Thesis, Catholic University of America (1970).
8. E. A. Spiegel and G. Veronis, On the Boussinesq approximation, *Astrophys. Jl* **131**(2), 443–447 (1960).
9. H. L. Kuo, On the dynamics of convective atmospheric vortices, *J. Atmos. Sci.* **23**, 25–42 (1966).
10. H. L. Kuo, Axisymmetric flows in the boundary layer of a maintained vortex, *J. Atmos. Sci.* **28**, 20–41 (1971).
11. J. Serrin, The swirling vortex, *Phil. Trans. Soc.* **271**, 325–360 (1972).
12. L. M. Gutman, Theoretical model of a waterspout, *Bull. Acad. Sci. USSR. Geophys. Ser.* **1**, 87–103 (1957).
13. V. M. Mal'bakhov, Investigation of the structure of tornadoes, *Izv. Atm. Ocean Phys.* **8**, 8–14 (1972).
14. W. Lewis and P. J. Perkins, Recorded pressure distribution in the outer portion of a tornado vortex, *Mon. Weath. Rev.* **81**, 379–385 (1953).
15. E. M. Sparrow and H. S. Yu, Local nonsimilarity thermal boundary layer solutions, *J. Heat Transfer* **93**, 328–334 (1971).
16. J.-M. Chen, A steady vortex driven by a line heat source—a possible model for the tornado, D. Eng. Dissertation, Tulane University (1974).
17. M. A. Goldschtik, A paradoxical solution of the Navier–Stokes equations, *Prikl. Mat. Mekh.* **24**, 913–929 (1960).
18. L. Rosenhead (editor), *Laminar Boundary Layers.* Clarendon Press, Oxford (1963).
19. E. M. Sparrow and W. J. Minkowycz, Local nonsimilar solutions for natural convection on a vertical cylinder, *J. Heat Transfer* **96**, 178–183 (1974).
20. J. S. Turner, The constraints imposed on tornado-like vortices by the top and bottom boundary conditions, *J. Fluid Mech.* **25**, 377–400 (1966).
21. G. F. Carrier, A. Hammond and O. George, A model of the mature hurricane, *J. Fluid Mech.* **47**, 145–170 (1971).
22. T. Fujita, 1959, Technical Report No. 5, A detailed analysis of the Fargo tornadoes of June 20, 1957, Technical Report No. 5, pp. 1–29, Severe Local Storm Project, University of Chicago (1959).
23. T. Fujita, Estimated wind speeds of the Palm Sunday Tornadoes, Satellite and Mesometeorology Research Project, Research Paper 53, University of Chicago, Dept. of Geophysical Science (April, 1967).
24. W. H. Hoecker, Wind speed and air flow patterns in the Dallas tornado and some resultant implications, *Mon. Weath. Rev.* **88**, 167–180 (1960).
25. H. L. Jones, A spheric method of tornado identification and tracking, *Bull. Am. Meteorol. Soc.* **32**, 380–385 (1951).

TOURBILLON STATIONNAIRE CREE PAR UNE SOURCE DE CHALEUR LINEAIRE

Résumé—On présente une analyse mathématique d'un tourbillon qui se forme au voisinage d'une source linéaire de chaleur avec une circulation constante loin de la source de chaleur et du sol. Les régions proches de l'axe du tourbillon et proches du sol, appelées respectivement région centrale et région de sol, sont traitées séparément en utilisant les approximations de couche limite. La présence du sol induit un puissant écoulement secondaire vers le centre du tourbillon et proche du sol. Les deux régions sont raccordées par des conditions de fluide non visqueux assez loin de l'axe du tourbillon et du sol, et en considérant les débits volumiques pour la couche limite de sol et pour la région centrale. La couche limite de sol a un effet important sur l'écoulement de la région centrale. Cet effet semble croître quand la viscosité diminue. Les résultats sont utilisés pour estimer l'intensité de la source énergétique nécessaire pour alimenter une tornade. Les résultats sont exploitables dans des phénomènes tels que les tourbillons de flamme et les tourbillons pilotés électriquement en laboratoire.

EIN STATIONÄRER DURCH EINE LINIENFÖRMIGE WÄRMEQUELLE INDUZIERTER WIRBEL

Zusammenfassung—Es wird die mathematische Behandlung eines Wirbels beschrieben, der sich um eine linienförmige Wärmequelle in einem Gebiet mit in weiter Entfernung von der Wärmequelle und der Grundfläche konstanter Zirkulation bildet. Die Gebiete in der Nähe der Mittellinie des Wirbels und an der Grundfläche, genannt der Kern bzw. das Grundflächengebiet, werden getrennt behandelt, wobei Grenzschichtnäherungsansätze benutzt werden. Durch die Anwesenheit der Grundfläche wird eine starke Sekundärströmung in Richtung des Zentrums des Wirbels in Wandnähe induziert. Die beiden Gebiete werden verknüpft durch Anpassen der Grenzbedingungen mittels eines reibungsfreien Zwischengebiets, das weit von der Mittellinie des Wirbels und der Wand entfernt ist und durch Gleichsetzen der Volumenströme, die an der Wandgrenzschicht in das Gebiet hinein und aufwärts in den Wirbelkern führen. Die Grenzschicht an der Wand hat einen großen Einfluß auf die Strömung im Kerngebiet. Der Einfluß scheint bei kleiner werdener Viskosität zuzunehmen. Die Ergebnisse werden benutzt, um die Intensität einer Energiequelle abzuschätzen, die erforderlich ist, um einen Tornado zu verursachen. Die Ergebnisse sind weiter nützlich bei der Analyse solcher Phänomene wie durch Feuer verursachter Wirbel und im Labor elektrisch induzierter Wirbel.

ДВИЖЕНИЕ СТАЦИОНАРНОГО ВИХРЯ ПОД ДЕЙСТВИЕМ ЛИНЕЙНОГО ИСТОЧНИКА ТЕПЛА

Аннотация — Представлено математическое описание формирования вихря от линейного источника тепла в области с заданной постоянной циркуляцией вдали от источника тепла и грунта. Области вблизи оси вихря и у грунта, названные, соответственно, областями ядра и грунта, рассматриваются отдельно в приближении пограничного слоя. Наличие грунта вызывает сильное вторичное течение к центру вихря вблизи грунта. Совмещение обеих областей проводится путём сращивания граничных условий через промежуточную область, находящуюся вдали как от оси вихря, так и от грунта, и на основе уравнивания объёмных расходов в направлении пограничного слоя на грунте и в направлении области ядра. Пограничный слой на грунте оказывает сильное влияние на область течения в ядре, причём тем большее, чем меньше вязкость жидкости. Результаты исследования используются для оценки интенсивности источника энергии, при которой происходит зарождение смерча. Кроме того, они могут оказаться полезными также для анализа таких явлений, как огневые вихри при пожарах и электрические вихри, генерируемые в лабораторных условиях.